Compact Inline E plane Waveguide Resonators and Bandpass Filters with I-shaped Resonant Insets

Jankovic, U. and Budimir, D.

This is a copy of the author's accepted version of a paper subsequently published in the proceedings of the *IEEE Asia Pacific Microwave Conference (APMC2016),* New Delhi, India, 05 to 09 Dec 2016.

It is available online at:

https://dx.doi.org/10.1109/APMC.2016.7931353

Proceedings of the Asia-Pacific Microwave Conference 2016

Compact Inline E-plane Waveguide Resonators and Bandpass Filters with I-shaped Resonant Insets

Uros Jankovic and Djuradj Budimir
Wireless Communications Research Group, FST, University of Westminster
London W1W 6UW, UK
d.budimir@westminster.ac.uk

***Abstract*- In this paper, waveguide resonators and bandpass filters with E-plane inserts containing I-shaped resonant insets are presented. These insets introduce to the response finite transmission zeros much less sensitive than those produced by cross-couplings. Also, their use results in structure compactness, unlike bandstop resonant cavities that add volume. Two kinds of extracted pole sections that demonstrate response flexibility of the proposed resonators are designed at 10 GHz and tested. One is based on the dominant mode with a transmission zero in the upper stopband and the other on a pair of higher order modes with a transmission zero in the lower stopband. Also, a 3rd order filter for 11 GHz band combining both dominant and higher order mode resonators is modeled to illustrate the scalability of such a modular design. These filters are very suitable for low-cost mass production.**

I. Introduction

Although waveguide technology had its initial most significant development during WWII within radar systems [1], and dual mode waveguide filters have become standard in satellite communications during 70s [2], it is still unequalled for low loss, high power and perfect electromagnetic isolation applications. Such are waveguide diplexers in modern base station transceivers [3] and new challenges are arising with system requirements like millimeter wave communication for 5G mobile networks [4]. Thus, a substantial research and development effort has been being given to reduce losses, improve compactness, passband flatness, stopband rejections, steepness of transition responses between passbands and stopbands and produce variety of frequency responses of waveguide filters to satisfy increasingly stringent specifications coming to the brink of the obtainable physical limits.

Konishi and Uenakada in [5] proposed use of a metal insert along waveguide E-plane for realization of directly coupled waveguide filters [6]. Likewise, E-plane waveguide technology is very suitable for implementation of ridged waveguide resonators [7] and quasi lowpass corrugated waveguide filters [8]. In [9], the size of the conventional E-plane resonator was reduced and transmission zero (TZ) introduced through the addition of metal S shaped lines on dielectric slab, and in [10] similar effect was created using fins. Additional complexity was introduced by using two parallel E-plane inserts [11], while generalized Chebyshev response was created through bypass coupling between the source and load.

In this paper, dielectric substrate has been maximally utilized to support balanced topology with centrally positioned floating I-shaped inset acting as a half-wavelength resonator to form a TZ antiresonance. Although the inset is simple enough to enable quick initial design, it has sufficient degrees of freedom for fine tuning to particular requirements. Another improvement is that high level of inset symmetry allows significant reduction of simulation time.

Loading a waveguide with a dielectric slab acts like adding central capacitance with ridges, lowering the cutoff frequency of the dominant mode, but not significantly affecting the next higher one, thus effectively increasing the bandwidth. Importantly, the power handling capacity is bigger for having higher dielectric strength material filling the space with the strongest field [12]. Compared to all-metal inserts, PCB manufacturing is generally more accessible and it removes response sensitivity to metal bending. Since waveguide filter housings are reusable and other waveguide components are standardized modules, the proposed filters have edge in ease of fabrication even over SIW and microstrip filters for neither needing vias nor soldering coaxial connectors.

II. Proposed Resonators

Configuration of an E-plane waveguide resonator with an I-shaped inset coupled on both sides to form an extracted pole section (EPS) is shown in Fig. 1a, whereas its equivalent circuit is depicted in Fig. 1b.

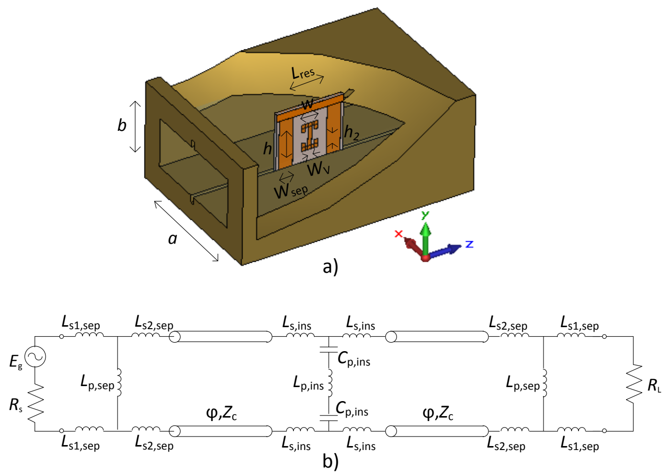

Figure 1. a) 3D model of the proposed E-plane resonator with I-shaped inset and b) its equivalent circuit.

The resonator structure has central x- and z-planes of symmetry, and essentially central y-plane as well, though the latter one is slightly violated in this implementation due to asymmetric position of the dielectric substrate. These properties are transposed into balanced symmetrical equivalent circuit.

For each resonator discontinuity inside the waveguide, its equivalent 2-port network is extracted from de-embedded center frequency Z-parameters of only that discontinuity independently full wave simulated in the waveguide. Equations $X_{s1} = \mathrm{Im}(z_{11} - z_{12})$, $X_{s2} = \mathrm{Im}(z_{22} - z_{12})$ and $X_p = \mathrm{Im}(z_{12})$ are applied to find X_{s1} and X_{s2} as serial reactances at ports 1 and 2 respectively and X_p as the parallel reactance of the equivalent T-network. This network is further transfigured into one of equivalent networks in Fig. 1b in a straightforward manner, with $L_{\mathrm{s,ins}}$ and $C_{\mathrm{s,ins}}$ satisfying the relation $f_z = 1/2\pi\sqrt{L_{\mathrm{s,ins}}\ C_{\mathrm{s,ins}}}$, where f_z is the frequency of the TZ produced by an independent I-shaped inset.

The physical length of I-shaped inset is shorter than half a wavelength due to the top and bottom widenings that represent capacitive loadings. Accordingly, the TZ position can be controlled by the inset height as well as by the sizes of loadings. The width of the line representing the loading has been fixed for all the presented designs here to be 0.8 mm. Smaller width has not been used to avoid problems with fabrication sensitivity. Described effect is similar to the one accomplished with adding capacitive loadings to a dipole antenna. Applying image theory across waveguide walls, the I-shaped insets can be transformed into 2D array of dipoles in the transverse *z*-plane.

The resonant frequency is, expectedly, controlled by the waveguide resonator length. (It is assumed that the waveguide profile is preselected.) The resonator response bandwidth is directed by the amount of coupling between source and load. A more narrowband response can be achieved through wider septa forming immitance inverters, but is produced by a wider I-shaped inset as well.

Sample structures have been designed at X band. Standard WR-90, (a x b) = (22.86 mm x 10.16 mm), rectangular waveguide made of brass ($\sigma_{\mathrm{Br}} = 15.9$ MS/m) with useful frequency band between 8.2 and 12.4 GHz is used. In the top and bottom waveguide walls along one side of the central E-plane are carved 1.5 mm deep and 0.8 mm wide grooves to hold a dielectric slab with etched metallization pattern. The housing itself is longitudinally split in two halves so that the slab can easily be put into the groove in one half and the other one can afterwards be screwed to the first one.

The slab is made out of $h_{\mathrm{sub}} = 0.79$ mm thick low loss ($\tan\delta = 0.0009$ at 10 GHz) Rogers RT/duroid 5880 high frequency laminate having relative permittivity $\varepsilon_r = 2.2$ [13]. Electrodeposited copper cladding is $t = 17$ µm thick with $R_q = 1.8$ µm RMS surface roughness on the dielectric side to result in effective conductivity of $\sigma_{\mathrm{Cu,clad}} = 15.4$ MS/m.

Propagation characteristics in the waveguide sections between the septa and the insets that are loaded with off-centered dielectric substrate can be found following the procedure outlined in [14]. In circuit simulation, they are modeled by standard TE_{10} mode sections with the waveguide width increased by 2.73 mm to match the phase constant and characteristic impedance of the actual distorted mode.

The PCB has been fabricated using LPKF ProtoMat C60 [15] circuit board plotter (Fig. 2). However, Rogers RT/duroid 5880 glass microfiber reinforced PTFE composite threaded structure does not appear to be particularly suitable for mechanical milling PCB fabrication, which has to a certain extent negatively affected the measured responses.

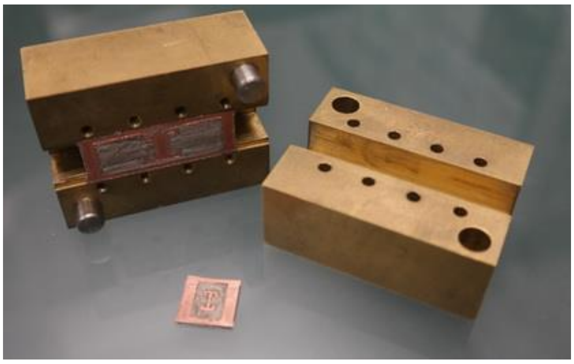

Figure 2. Photograph of the two fabricated resonator inserts with the brass waveguide housing.

A. *Dominant Mode Resonator*

The dominant mode is based on the TE_{101} rectangular cavity mode. This can be verified by inspecting standing wave patterns in field distribution and by the resonant frequency shifts while altering different resonator dimensions. The electromagnetic field is predictably the strongest in the resonator center region around the inset. Apart from determining the TZ location, the I-shaped inset size affect the transmission pole (TP) location as well since it effectively meanders the EM field inside the resonant cavity. Moreover, the increase in its size more rapidly decreases the resonant frequency than additional cavity length, helping to drastically shrink the resonator size.

In Fig. 3 is given simulated response from CST MICROWAVE STUDIO [16] of a dominant TE_{101} mode resonator with physical lengths and values of equivalent circuit lumped elements listed in the table I, referring to the dimensions described in Fig. 1. It can be concluded that size reduction of 35% has been achieved compared to the conventional E-plane filter with the same implementation. Between the septum and the inset, the energy is mostly carried by TE_{n0} modes, n = 1, 3, 5, …, where each higher modes decreases about 10 dB in intensity. When no additional coupling between discontinuities is modeled, TZ frequency is about 6% higher than its real value, whereas TP frequency is only about 1.5% below 10 GHz. The response of the fabricated dominant mode resonator was measured using Agilent E8361A PNA Network Analyzer, and is also presented in Fig. 3 for comparison.

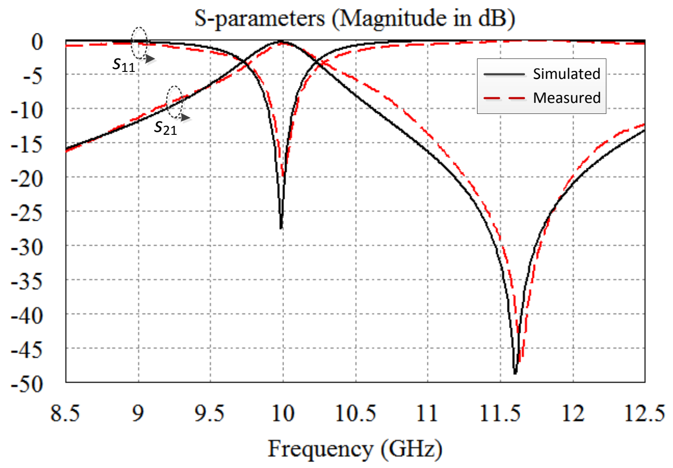

Figure 3. Simulated and measured transmission and reflection S- parameters of the dominant mode resonator.

TABLE I.
DIMENSIONS OF THE EPS WITH THE DOMINANT MODE RESONANCE AND EQUIVALENT CIRCUIT LUMPED ELEMENT VALUES

Dimension	L_{res}	W_{sep}	W_V	h	h_2	w
Length [mm]	7.0	2.9	0.8	5.6	1.7	3.4
Element	$L_{s1,sep}$	$L_{s2,sep}$	$L_{p,sep}$	$L_{s,ins}$	$L_{p,ins}$	$C_{p,ins}$
Value [nH/µF]	2.24	1.29	3.39	2.13	8.51	$3.9e^{-8}$

Unloaded Q factor was calculated to be 1873 using eigenmode solver in CST MICROWAVE STUDIO. I-shape inset dimensions were kept constant while completely closing the resonator couplings and finding the new resonator length to be 12.1 mm so that the resonant frequency of the dominant mode is exactly 10 GHz. Q_u is calculated by perturbation method, having Q factor due to conductor (surface) losses $Qc = 6517$ and Q factor due to dielectric (volume) losses $Qd = 2628$, in total giving $\frac{1}{Q_u} = \frac{1}{Q_c} + \frac{1}{Q_d}$.

B. *Higher Order Dual Mode Resonator*

First two higher order modes are another variations of TE_{102} and TE_{103} rectangular cavity modes. Since the field distribution of TE_{103} mode has maximum in the cavity center, whereas TE_{102} mode has minimum, the I-shaped inset considerably more affects the TE_{103} mode than the TE_{102} mode. Hence, the distance between the two TPs can be adjusted with the inset. The simulated and measured responses of the resonator accommodating these two modes are shown in Fig. 4 with dimensions and circuit element values listed in the table II, referring to the dimensions described in Fig. 1. In this case, when no additional coupling between discontinuities is modeled, TZ frequency is about 15% lower than its real value. At the same time, TP frequency has much smaller shift of around 3% downwards.

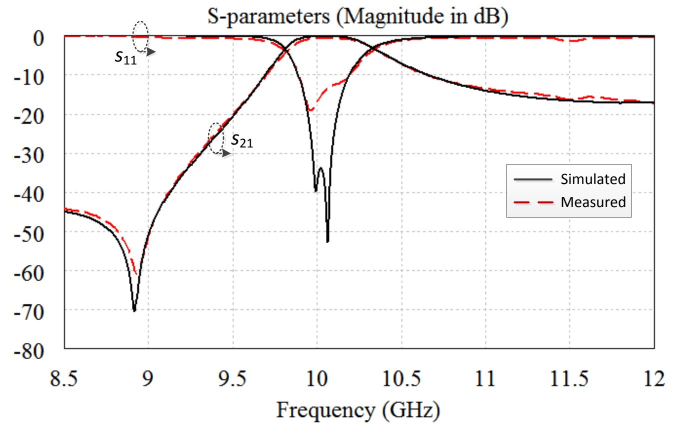

Figure 4. Simulated and measured transmission and reflection S-parameters of the higher order dual mode resonator.

TABLE II.
DIMENSIONS OF THE EPS WITH THE HIGHER MODE RESONANCES AND EQUIVALENT CIRCUIT LUMPED ELEMENT VALUES

Dimension	L_{res}	W_{sep}	W_V	h	h_2	w
Length [mm]	30.4	2.9	4.2	8.8	2.4	8.6
Element	$L_{s1,sep}$	$L_{s2,sep}$	$L_{p,sep}$	$L_{s,ins}$	$L_{p,ins}$	$C_{p,ins}$
Value [nH/µF]	2.24	1.29	3.39	5.86	7.79	$8.1e^{-8}$

For TE_{103} mode, $Q_u = 2610$ with $Qc = 5330$ and $Qd = 5114$ ($L_{res} = 35.1$ mm). In the case of TE_{102} mode, $Q_u = 2821$ with $Qc = 4586$ and $Qd = 7327$ ($L_{res} = 37.6$ mm)

III. FILTERS WITH I SHAPED RESONANT INSETS

A 3rd order E-plane filter with I-shaped insets is designed by cascading one section of dominant mode resonator and one section of dual mode cavity with higher order modes. In Fig. 5 is presented the layout of the filter insert, and in table III dimension for such a filter having the passband at 11 GHz.

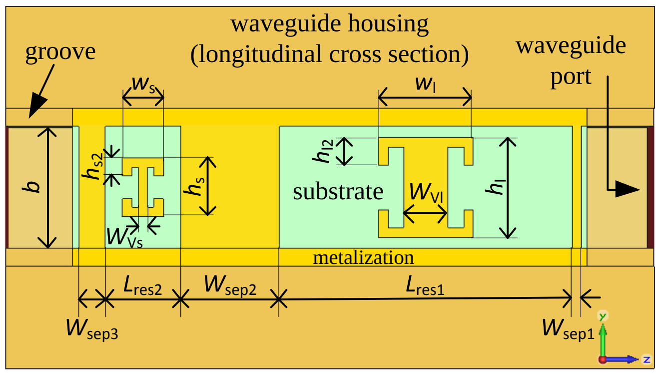

Figure 5. Longitudinal cross section of a 3rd order filter.

TABLE III.
DIMENSIONS OF THE 3RD ORDER FILTER

Dimension	Length [mm]	Dimension	Length [mm]
L_{res1}	24.4	h_{l}	8.3
L_{res2}	6.3	h_{l2}	2.3
W_{sep1}	0.7	w_{l}	7.9
W_{sep2}	8.2	h_{s}	4.9
W_{sep3}	2.2	h_{s2}	1.5
W_{Vl}	3.7	w_{s}	3.4
W_{Vs}	0.8		

In Fig. 6 are displayed S-parameters of the proposed 3rd order filter with generalized Chebyshev response simulated in CST MICROWAVE STUDIO. Although the structure is not symmetric, the difference between the two reflection parameters is minuscule, so s_{22} parameter is not presented for the clarity purpose.

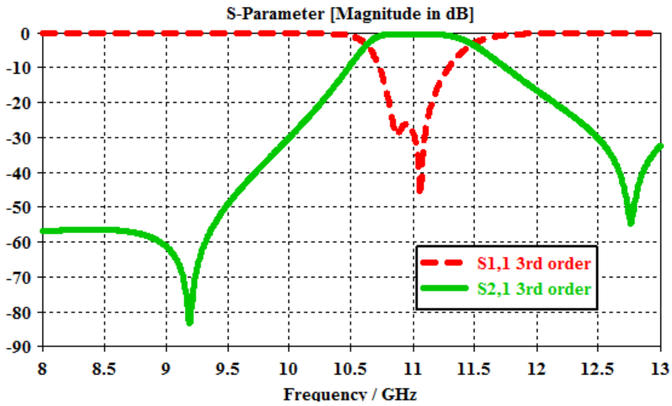

Figure 6. Transmission and reflection S-parameters of the 3rd order filter.

From the simulation results it can be observed that reflection loss is better than 20 dB in the frequency range between 10.808 GHz and 11.154 GHz and in the same range insertion loss is less than 0.4 dB. On the other side, 3db bandwidth is between 10.625 GHz and 11.482 GHz. This effect of having quite different center frequencies when using two different criteria for the passband can be attributed to much steeper roll-off in the lower passband than in the upper one. Differences in passband to stopband transition steepness is due to the waveguide behaving as a high-pass filter, in addition to having spurious passbands at higher frequencies where the filter discontinuities cease to reflect higher order waveguide modes. Thus, to have more symmetric response it is necessary to introduce higher number of transmission zeros in the upper stopband.

IV. CONCLUSION

A new type of compact size E-plane waveguide filters with quasi-elliptic response and inline geometry has been proposed. Resonators with I-shaped resonant insets designed at 10 GHz have Q factors of 1873, 2610 and 2821 for the first three modes respectively. The resonators have been verified by measurement and equivalent circuits aimed for synthesis procedure developed and their accuracy investigated. By producing transmission zeros at both 11.6 GHz and 8.85 GHz is demonstrated possibility of introducing steep transition by a reflection pole in either upper or lower stopband. In addition, a 3rd order filter having all presented cavity modes was modeled for 11 GHz center frequency, with total length of 41.8 mm being 23% shorter than its conventional all-pole E-plane counterpart. Its simulated insertion loss in the passband is only 0.4 dB.

REFERENCES

[1] Volume 1-27, *MIT Radiation Laboratory Series*, McGraw-Hill, New York, 1947.

[2] A. E. Atia, A. E. Williams, "Narrow-Bandpass Waveguide Filters," *IEEE Trans. Microw. Theory Tech.*, vol.20, no.4, pp.258-265, Apr 1972.

[3] G. Macchiarella and S. Tamiazzo, "Design of "Masthead" Combiners," *2015 European Microwave Conference*, 2015, pp. 686–689.

[4] C. Dehos, J. L. González, A. D. Domenico, D. Kténas, and L. Dussopt, "Millimeter-wave access and backhauling: the solution to the exponential data traffic increase in 5G mobile communications systems?," *IEEE Commun. Mag.*, vol. 52, no. 9, pp. 88–95, Sep. 2014.

[5] Y. Konishi and K. Uenakada, "The Design of a Bandpass Filter with Inductive Strip - Planar Circuit Mounted in Waveguide," *IEEE Trans. Microw. Theory Tech.*, vol. 22, no. 10, pp. 869–873, Oct. 1974.

[6] S. B. Cohn, "Direct-Coupled-Resonator Filters," *Proc. IRE*, vol. 45, no. 2, pp. 187–196, Feb. 1957.

[7] Djuradj Budimir, *Generalized filter design by computer optimization*, Boston, Mass; London: Artech House, 1998.

[8] G. Goussetis and D. Budimir, "Novel periodically loaded E-plane filters," *IEEE Microwave Wireless Components Lett.*, vol. 13,no. 6, pp. 193–195, Jun. 2003.

[9] S. Niranchanan, A. Shelkovnikov, and D. Budimir, "Novel millimetre wave metawaveguide resonators and filters," *2007 European Microwave Conference*, 2007, pp. 913–916.

[10] O. Glubokov and D. Budimir, "Extraction of Generalized Coupling Coefficients for Inline Extracted Pole Filters With Nonresonating Nodes," *IEEE Trans. Microw. Theory Tech.*, vol. 59, no. 12, pp. 3023–3029, Dec. 2011.

[11] N. Mohottige, U. Jankovic, and D. Budimir, "Ultra compact pseudo-elliptic inline waveguide bandpass filters using bypass coupling," *IEEE MTT-S International Microwave Symposium (IMS)*, June 1- 6, 2014, Tampa, Florida, USA.

[12] W. P. Ayres, P. H. Vartanian, and A. L. Helgesson, "Propagation in Dielectric Slab Loaded Rectangular Waveguide," *IRE Trans. Microw. Theory Tech.*, vol. 6, no. 2, pp. 215–222, Apr. 1958.

[13] https://www.rogerscorp.com/

[14] N. Eberhardt, "Propagation in the Off Center E-Plane Dielectrically Loaded Waveguide," *IEEE Trans. Microw. Theory Tech.*, vol. 15, no. 5, pp. 282–289, May 1967.

[15] http://www.lpkf.com/

[16] http://www.cst.com/